Dynamic Properties of the Phosphorescent Triplet State of 9*H*-Thioxanthen-9-one (Thioxanthone) from Optically Detected Magnetic Resonance Spectroscopy

Kazuhiko SUGA and Minoru KINOSHITA*

The Institute for Solid State Physics, The University of Tokyo, Roppongi, Minato-ku, Tokyo 106

(Received December 10, 1980)

A variety of optically detected magnetic resonance (ODMR) experiments have been performed on the lowest excited triplet state of 9*H*-thioxanthen-9-one at 1.4 K. The absorption and phosphorescence excitation spectra were also measured to supplement the ODMR studies. The results were analyzed to determine the mechanisms responsible for the radiative decay and intersystem crossing processes. The z sublevel has large activity in vibronic bands due to non-totally symmetric vibrations. The intensity mainly comes from mechanisms involving vibronic coupling between $^1n,\pi^*$ and $^1\pi,\pi^*$ states. The y sublevel is selectively affected by the introduction of the sulfur atom, because of the increased importance of spin orbit coupling with $^1\sigma',\pi^*$ state which is largely localized on the thioether group.

Detailed information about the magnetic and spectroscopic properties of the lowest triplet states of aromatic carbonyls[1-13] has been accumulated in recent years, particularly by means of optically detected magnetic resonance (ODMR) spectroscopy. In the case of aromatic carbonyls having the lowest triplet states of π,π^* type, these properties have been shown to vary markedly depending on the molecular structure, the nature of environments, and the energy separations between the $^3\pi,\pi^*$ state and $^3n,\pi^*$ state (ΔE_{TT}) or the $^1n,\pi^*$ state (ΔE_{ST}). However, in the case of 9*H*-xanthen-9-one (we shall use the popular name, xanthone, hereafter) where ΔE_{TT} is rather large and the carbonyl group is rigidly held to the planar π-electron system, Chakrabarti and Hirota[17] have shown that the radiative and non-radiative properties are very different from those found in other carbonyls such as benzaldehydes and acetophenones.

The aims of the present paper are to study dynamic properties of the lowest triplet state of 9*H*-thioxanthen-9-one (we shall use the popular name, thioxanthone, hereafter) in comparison with those of xanthone[14-19] and to elucidate the mechanism of dynamical processes of the state.

Experimental

Xanthone, thioxanthone, and bis(4-bromophenyl) ether (DDE) were purified by recrystallization followed by extensive zone refining under vacuum. Hexane, heptane, and octane of spectroscopic grade (Tokyo Kasei Co., Ltd.) were used without further purification. Crystals were grown by the Bridgman method from the melts.

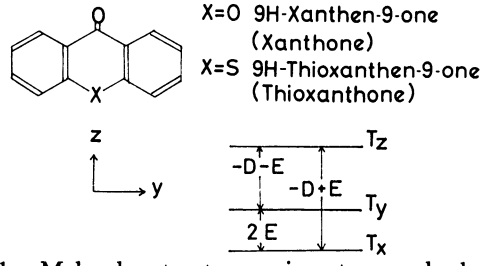

Fig. 1. Molecular structure, axis system, and scheme of zero field splitting.

The experimental set up for optical and magnetic resonance spectroscopic experiments was essentially the same as that reported previously.[20,21] The absorption spectra were measured on solutions in 1 cm path quartz cells by a Hitachi type 556 spectrophotometer at room temperature.

The molecular structures of xanthone and thioxanthone are shown in Fig. 1 together with the axis system used in this study and the zero-field(zf) splitting pattern which will be described below.

Results

Absorption Spectra. Figure 2 shows the absorption spectrum of thioxanthone observed in hexane at room temperature in comparison with that of xanthone. The intensity of the whole spectrum of thioxanthone is approximately halved as compared with that of xanthone, and each band shifts by about 3000 cm^{-1} to the red, showing that the excited π,π^* states lower their energy by sulfur substitution.

Phosphorescence Excitation Spectra. The phosphor-

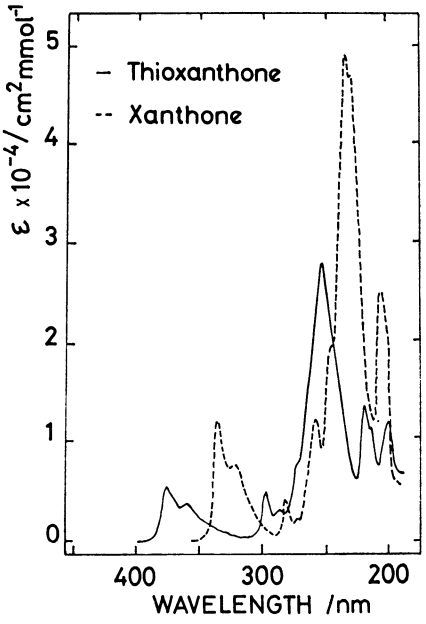

Fig. 2. The absorption spectra of thioxanthone (——) and xanthone (- - - -) in hexane at room temperature.

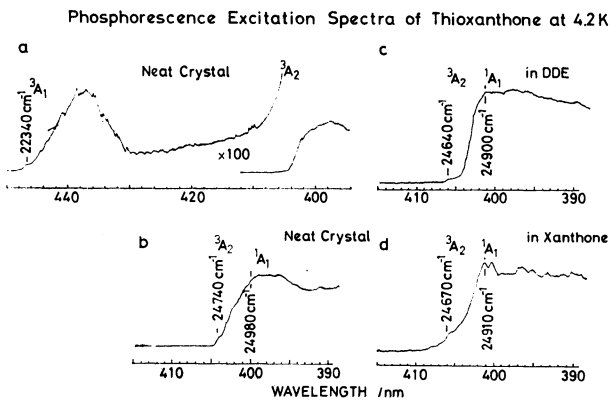

Fig. 3. The phosphorescence excitation spectra of thioxanthone at 4.2 K.
a) and b) neat crystal, c) in DDE, and d) in xanthone.

escence excitation spectra of thioxanthone in several host crystals are shown in Fig. 3. The excitation spectrum of the thioxanthone neat crystal starts at 22340 cm^{-1}, which is about 60 cm^{-1} higher than that of the origin of the phosphorescence spectrum. This indicates that the phosphorescence of the neat crystal, to be discussed below, originates from traps. There are a strong absorption band at 24980 cm^{-1} and a shoulder at about 24740 cm^{-1}. In the DDE and xanthone host crystals, the absorption at 22340 cm^{-1} is not observable, but other two absorption bands are clear.[22] The absorption at 24980 cm^{-1} is assigned to the $^1A_1(\pi,\pi^*)\leftarrow S_0$ absorption by considering the position of the first band in Fig. 2 and the excitation spectrum in heptane shown in Fig. 4. The absorptions starting at 24740 and 22340 cm^{-1} are assigned to the transitions of $^3A_2(n,\pi^*)\leftarrow S_0$ and $^3A_1(\pi,\pi^*)\leftarrow S_0$, respectively.

The excitation spectra of thioxanthone obtained in normal alkanes are complicated because of superposition of the spectra coming from multiple sites. The spectra coming from the sites are separated by using site selective monitoring technique. As an example, the spectra of the two major sites in heptane are shown in Fig. 4. The site higher in energy is referred to as site I, and the site lower as site II.

The phosphorescence excitation spectrum obtained in hexane is also shown in Fig. 5. Table 1 compares

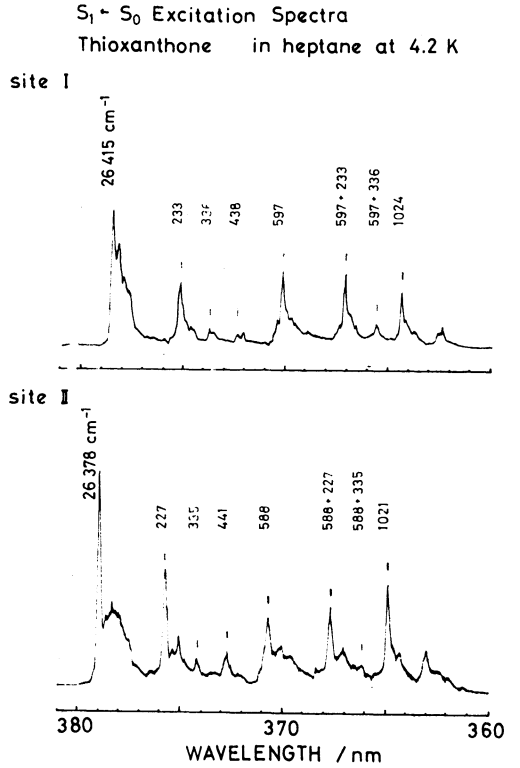

Fig. 4. The single site excitation spectra of thioxanthone in heptane at 4.2 K.
Site I (upper) and site II (lower).

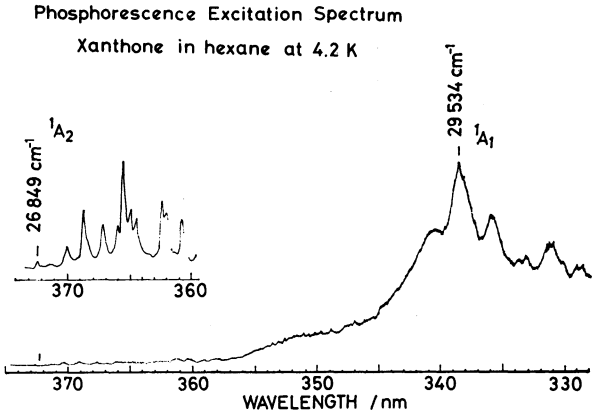

Fig. 5. The phosphorescence excitation spectrum of xanthone in hexane at 4.2 K.

TABLE 1. THE ENERGY LEVELS OF LOWER LYING EXCITED STATES AND THE ENERGY SEPARATIONS BETWEEN $^3\pi, \pi^*$ AND $^3n, \pi^*$ STATES (ΔE_{TT}) AND BETWEEN $^3\pi, \pi^*$ AND $^1n, \pi^*$ STATES (ΔE_{ST}) (IN UNITS OF cm^{-1})

	Thioxanthone				Xanthone	
	in neat crystal	in DDE	in xanthone	in hexane	in neat crystal	in hexane
$^3\pi, \pi^*$ (A_1)	22 340	22 270[a]	22 280[a]	23 215[a]	25 228	25 723[a]
$^3n, \pi^*$ (A_2)	24 740	24 640	24 670		26 689	
$^1n, \pi^*$ (A_2)					27 750	26 848
$^1\pi, \pi^*$ (A_1)	24 980	24 900	24 910	26 437		29 534
ΔE_{TT}	2400	2360	2390		1461	very small
ΔE_{ST}	>2640	>2630	>2630	>3222	>2522	1125

a) Obtained from the phosphorescence spectra. Others were determined from the phosphorescence excitation spectra.

the locations of the lower lying excited states of xanthone and thioxanthone determined from the excitation spectra. The energy levels for xanthone are essentially identical with those reported.[14,17] Most results for thioxanthone are new.

ODMR Experiments. Two strong MIDP signals at 3.088 and 1.098 GHz were observed for the emission of the traps in the thioxanthone neat crystal. Third zf transition at about 1.99 GHz could be observed by monitoring the emission at the 0,0 band. In view of the results of the other $^3\pi,\pi^*$ aromatic carbonyls so far studied,[1-9] the ordering of the sublevels is reasonably assigned as $T_z > T_y > T_x$ in energy. The x sublevel is the slowest decaying one. This assignment will be verified further by the unique behavior of the middle sublevel. Therefore, the zf transitions at 3.088 and 1.098 GHz are assigned as the $T_z \leftrightarrow T_x$ and $T_y \leftrightarrow T_x$ transitions, respectively. The ODMR transitions of thioxanthone observed in the DDE and xanthone host crystals are also assigned in a like manner. It is worthy to note that in the case of these three crystal systems, the total decay rates of the y and z sublevels are almost similar and large.

In the case of thioxanthone in hexane, on the other hand, only two positive PMDR signals were observed at 1.179 and 1.373 GHz. The third transition could be observed only slightly by the MIDP method at about 2.6 GHz. Since there is a strong likelihood that the x sublevel is the slowest decaying one, the signal at 1.179 GHz is attributed to the $T_y \leftrightarrow T_x$ transition and the signal at 1.373 GHz to $T_y \leftrightarrow T_z$. Two different sets of the zf ODMR transitions were observed for thioxanthone in heptane. The site selective experiment leads to the conclusion that site I is associated with the transitions at 1.186 and 1.376 GHz, and site II at 1.176 and 1.373 GHz.

The two sets of the ODMR signals corresponding to two distinct emitting species were observed for xanthone in the DDE host. The properties of these emitting species in the DDE host are very similar to those of the two traps observed in the xanthone neat crystal.[17]

The total decay rates k_i, relative steady state populations N_i^0, and relative populating rates P_i of the spin sublevels (i=x, y, z) were measured by the MIDP method. The relative radiative decay rates k_i^r were obtained for the 0,0 and vibronic bands at 0—670 cm^{-1}. The results are summarized in Table 2.

Phosphorescence and Sublevel Emission Spectra. The phosphorescence spectra of thioxanthone in alkanes were obtained under steady state excitation conditions. The spectrum obtained in hexane is shown in Fig. 6 in comparison with that of xanthone. The latter is resolved much better than the spectrum in the literature.[18] Unlike in hexane, where only one major site is evident, the phosphorescence spectra in heptane and octane appear as no less than two-site emission.

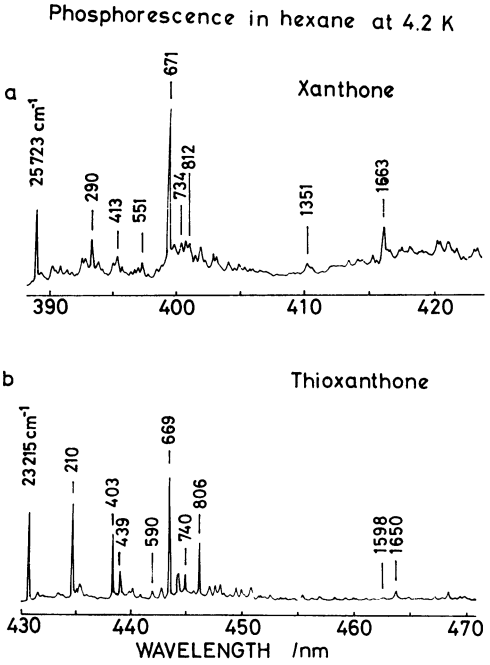

Fig. 6. The phosphorescence spectra in hexane at 4.2 K. a) Xanthone and b) thioxanthone.

Table 2. The kinetic and magnetic properties of the spin sublevels of $^3\pi, \pi^*$ states of xanthone and thioxanthone

	Thioxanthone						Xanthone in DDE	
	traps in crystal	in DDE	in xanthone	in hexane	in heptane Site I	in heptane Site II	Site I	Site II
$\|D\|/cm^{-1}$	0.0847	0.0825	0.0853	0.0655	0.0657	0.0654	0.1352	0.1111
$\|E\|/cm^{-1}$	0.0183	0.0185	0.0177	0.0197	0.0197	0.0196	0.0181	0.0188
k_z/s^{-1}	10.5	9.8	10.2	1.28	1.51	1.56	12.0	15.0
k_y/s^{-1}	12.1	10.5	9.4	9.9	8.2	9.5	1.70	1.42
k_x/s^{-1}	0.26	0.31	0.31	0.78	1.23	1.23	0.77	0.50
$P_z/\%$	51	54	57	23	33	31		
$P_y/\%$	47	43	40	59	43	49		
$P_x/\%$	2	3	3	18	24	20		
k_z^r/k_y^r 0[a]	0.06	0.10	0.11	0.13	0.02	0.06	1.2	1
670[b]	0.70	1.10	1.13	0.38	0.15	0.22	5.5	8.3
k_x^r/k_y^r 0[a]	0.01	0.01	0.01	0.08	0.03	0.04		
670[b]	0.02	0.04	0.05	0.24	0.11	0.16	0.20	0.31

a) Ratio obtained at the 0—0 band. b) Ratio obtained at the 0—670 cm^{-1} band.

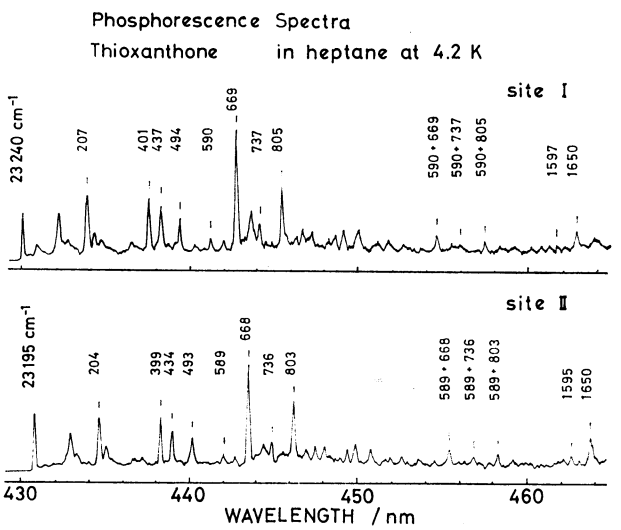

Fig. 7. The single site phosphorescence spectra of thioxanthone in heptane at 4.2 K.
Site I (upper) and site II (lower).

As an example, the emission spectra of sites I and II in heptane obtained by using the site selective excitation technique are shown in Fig. 7.

Much clear information can be obtained through separated sublevel emission spectra measured by means of the MIDP spectrum method reported previously.[20] Figure 8 shows the sublevel emission spectra of thioxanthone in hexane. Vibrational analysis of the spectrum is made by reference to the vibrational data for the compounds with related structure.[26-28] The vibronic bands found at 0—1650 and 0—1598 cm^{-1} are due to the C=O and C=C stretching modes of a_1 symmetry, respectively. The band at 0—590 cm^{-1} is also due to the totally symmetric mode, the combinations of which with the other modes have a certain intensity in the phosphorescence spectrum.

By considering the intensity behavior, the rest of bands of a considerable intensity may be attributed to the non-totally symmetric modes. The vibrations such as 670 and 810 cm^{-1} are considered as the same

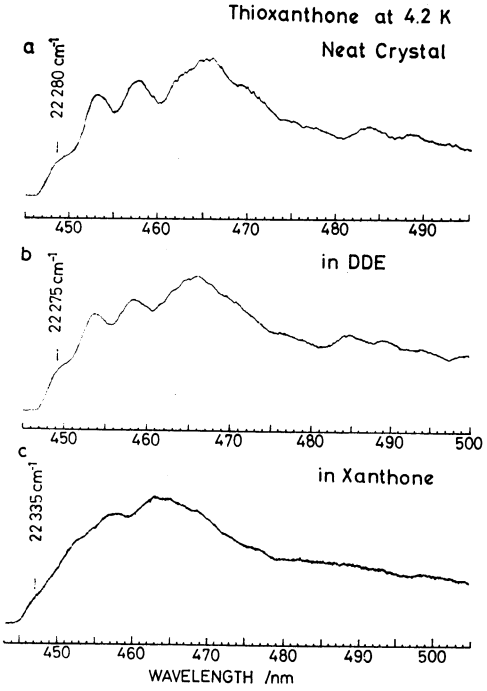

Fig. 9. The phosphorescence spectra at 4.2 K.
a) Thioxanthone traps in the neat crystal, b) thioxanthone in DDE, and c) in xanthone.

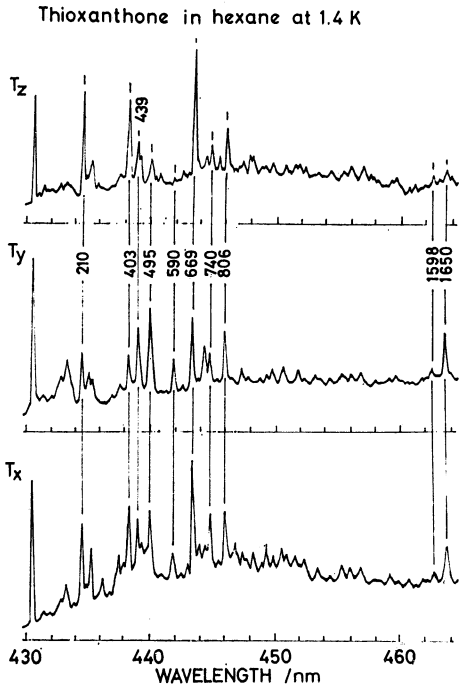

Fig. 8. The sublevel phosphorescence spectra of thioxanthone in hexane at 1.4 K.

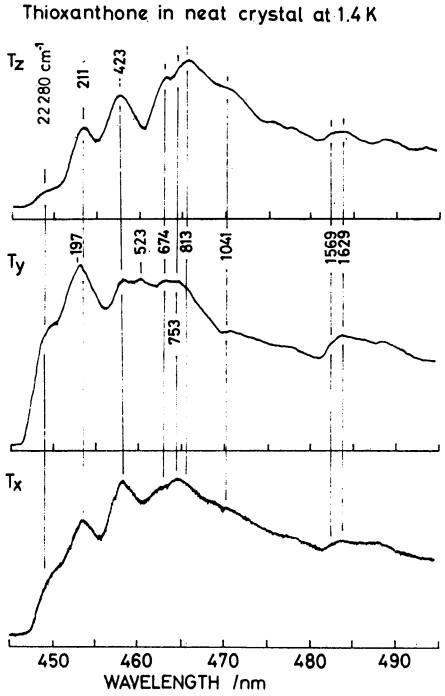

Fig. 10. The sublevel phosphorescence spectra of thioxanthone traps in the neat crystal at 1.4 K.

vibrations appearing in the spectrum of xanthone. In view of the infrared activity,[28] these vibrations are surely assigned to the out of plane vibrations of b_1 symmetry in the case of xanthone. The vibrational modes such as 430 and 720 cm^{-1}, more intense in the y sublevel spectrum than z, may be considered also as the out of plane vibrations probably of a_2 symmetry.

The phosphorescence spectra of thioxanthone also obtained in various crystals are shown in Fig. 9. The sublevel emission spectra obtained for traps in the neat crystal are shown in Fig. 10. The vibrational modes of 211, 423, 674, and 813 cm^{-1}, corresponding to frequencies 210, 403, 669, and 813 cm^{-1} observed in hexane, also appear in the z sublevel spectrum.

The phosphorescence spectra of xanthone are measured in alkanes and in the DDE host crystal. Although the spectra in heptane and octane appear as multi-site emission, the vibrational feature is very similar to that in hexane, shown in Fig. 6. As in the case of the xanthone neat crystal,[17] the phosphorescence spectrum in DDE appears to consist of the superposition of the spectra with different origins, one at 25023 cm^{-1} and the other at 24890 cm^{-1}.

Discussion

Total Decay Rate and Zero Field Splitting. The decay rate of the y sublevel, $k_y=12.1\ s^{-1}$, for traps in the thioxanthone neat crystal is larger by a factor of about six than that for traps in the xanthone neat crystal.[17] Such a remarkable change in the decay rate of the y sublevel must be due to the heavier nucleus S instead of O. In fact, the effective one electron spin orbit coupling constant for the 3p electrons of a S atom is expected to be much larger than that for the 2p electrons of an O atom.[25] Accordingly, the mixing with a $^1B_1(\sigma',\pi^*)$ state which is largely localized on the ether or thioether group may play a considerable role in determining k_y's of both compounds in addition to the mixing with the $^1B_1(\sigma,\pi^*)$ state, largely localized on the carbonyl group. This conclusion may be supported by the fact that the value of k_y of xanthone is considerably larger than the decay rates due to the mixing with $^1\sigma,\pi^*$ state commonly found in other systems such as quinoxaline[23] and naphthalene.[24] Furthermore, the above consideration confirms the assignment of the middle sublevel to y and verifies the zf splitting pattern of Fig. 1.

In the systems of thioxanthone traps in the neat, DDE, and xanthone crystals, the decay rates of the x sublevel are considerably smaller as compared with those of substituted benzaldehydes.[1,7,8] This seems to indicate that neither the $^3n,\pi^*$ admixture into the lowest $^3\pi,\pi^*$ state *via* vibronic coupling nor the deviation from the planarity contributes to k_x. A similar conclusion has been obtained for xanthone in crystalline hosts.[17] In the systems of thioxanthone in alkanes, however, relatively large values of k_x are obtained. The reason for this is not clear at present, but a possible contribution from spin-lattice relaxation is not completely eliminated in the alkane systems.

In xanthone it was shown that spin orbit mixing with $^1n,\pi^*$ state is mainly responsible for the decay from the z sublevel, because rather large ΔE_{TT} is unfavorable for mixing with $^3n,\pi^*$ state.[17] This is also true for thioxanthone. Both ΔE_{TT} and ΔE_{ST} become large by introduction of sulfur instead of oxygen. However, the decrease in k_z observed in the thioxanthone neat crystal is not so large as that expected from the increase in ΔE_{TT} and rather seems to reflect the increase in ΔE_{ST}. Therefore, rather small difference in k_z between xanthone and thioxanthone observed in the neat crystals seems to confirm the above inference.

It is notable that the total decay rates of the z sublevel of thioxanthone in alkanes are much smaller than those obtained in the crystal systems, clearly indicating that the mixing with $^1n,\pi^*$ state is reduced largely in hexane. This may be a consequence of larger value of ΔE_{ST} and/or smaller value of spin orbit matrix element, $G=\langle\pi,\pi^*|H_{SO}|n,\pi^*\rangle$, than in crystal system.

The $|D|$ values of thioxanthone traps in the neat crystal and in the DDE and xanthone hosts are small compared with that of xanthone.[17] By assuming that the value of the spin orbit coupling matrix element, G, is similar to that estimated for a series of benzaldehydes; $G^2=90\ cm^{-2}$,[5,8] the difference in the spin orbit contribution to D of xanthone and thioxanthone is predicted to be about 0.037 cm^{-1}. This value seems to be in agreement with the observed difference in D. Thus, the change in the spin orbit contribution is responsible, at least partly, for the change in D. Further reduction in $|D|$ observed when the environment is changed to alkanes suggests that the energy difference, ΔE_{TT}, becomes much larger in these matrices.

Intersystem Crossing. There is a distinct difference in the populating rates between the systems of thioxanthone in alkanes and in the other host crystals. Since the lowest excited triplet and singlet states of thioxanthone are π,π^* states of A_1 orbital symmetry, all the three sublevels require vibronic spin orbit mechanisms, when the intersystem crossing is assumed to proceed directly from S_1 to T_1. However, if the $T_2(n,\pi^*)$ state lies lower than S_1, it is necessary to consider an indirect process, namely $S_1\rightarrow T_2\rightarrow T_1$, which may make a contribution toward populating of the z sublevel.

In the case of thioxanthone traps in the neat crystal and in the DDE and xanthone hosts, the populating pattern of the sublevels is characterized by high selectivity for the y and z sublevels, relative to the x sublevel. In these host crystals, the $T_2(n,\pi^*)$ state is located lower than S_1. The high selectivity for the z sublevel, therefore, indicates clearly that the indirect process plays a role in the populating process of the z sublevel.

In the case of thioxanthone in hexane and heptane, on the other hand, ΔE_{TT} is much larger than in the DDE and xanthone host crystals, as described in the preceding section. As a result, the T_2 and S_1 states are expected to interchange position. If this is the case, the significant decrease in the relative populating rate of the z sublevel on going from in the host crystals to in alkanes is surely ascribed to the vanishment of the indirect process and also to the decrease of the vibronic interaction between the n,π^* and π,π^* states in singlet and/or triplet manifolds resulting from the increase of the energy separations.

As discussed in the preceding section, there is a good reason to expect that the mixing between the $^3A_1$ and $^1B_1(\sigma',\pi^*)$ states is effective. In addition, there is also evidence for considerably large b_1 vibration band activity in the y sublevel emission (Table 2). Thus, the large activity of the y sublevel with respect to the intersystem crossing process can be interpreted as a consequence of, for the main, large spin orbit coupling terms between the $^3A_1$ and $^1B_1(\sigma',\pi^*)$ states and also vibronic coupling matrix element between the $^1A_1$ and $^1B_1$ states.

Radiative Processes. Radiative Decay from the z Sublevel: The mechanisms governing the radiative decay from the z sublevel of $^3\pi,\pi^*$ aromatic carbonyls so far studied[7,8,10-13] may be classified as follows.

(1) Direct spin orbit mixing with the $^1n,\pi^*$ state

$$T_z(^3\pi,\pi^*) \leftarrow H_{so} \rightarrow {}^1n,\pi^*$$

(2) Direct configurational mixing with the $^3n,\pi^*$ state

$$T_z(^3\pi,\pi^*) \leftarrow H_{el} \rightarrow T_z(^3n,\pi^*) \leftarrow H_{so} \rightarrow {}^1\pi,\pi^*$$

(3) Herzberg-Teller type vibronic spin orbit mixing

(a) $T_z(^3\pi,\pi^*) \leftarrow H_v \rightarrow T_z(^3n,\pi^*) \leftarrow H_{so} \rightarrow {}^1\pi,\pi^*$

(b) $T_z(^3\pi,\pi^*) \leftarrow H_{so} \rightarrow {}^1n,\pi^* \leftarrow H_v \rightarrow {}^1\pi,\pi^*$

It has been shown that the relative importance of these is much dependent on the systems chosen.

In xanthone, Chakrabarti and Hirota[17] have shown that mechanisms (1), (2), and (3a) are not main ones and that only mechanism (3b) may be considered to be important for the emission of the z sublevel. A similar conclusion holds commonly for thioxanthone, but some more detailed information can be obtained by comparing the results with those of xanthone.

Mechanism (1) is important rather than mechanism (2) in the 0,0 band emission from the z sublevel. This inference can be derived from the facts that the relative intensity of the 0,0 band in the z sublevel emission is insensitive to the change in ΔE_{TT} from 1461 cm^{-1} for xanthone to 2400 cm^{-1} for thioxanthone and that the z sublevel emits only weakly at the 0,0 band even in the system of xanthone in hexane where ΔE_{TT} is relatively small.

With respect to xanthone, Chakrabarti and Hirota have suggested, on the basis of the phosphorescence polarization data by Pownall and Huber,[14] that such strong bands as found at 0—670 cm^{-1} likely gain intensity by the following mechanism.[17]

$$T_z(^3\pi,\pi^*) \leftarrow H_{so} \rightarrow {}^1n,\pi^*(A_2) \leftarrow H_v(b_1) \rightarrow {}^1\pi,\pi^*(B_2)$$

As mentioned above, the out of plane vibrational modes such as 670 and 810 cm^{-1} of thioxanthone can be assigned to the vibrations of b_1 symmetry. The observation that these vibrations appear strongly in the z sublevel spectra of thioxanthone seems to give a good proof of the validity of the mechanism suggested by Chakrabarti and Hirota.

The a_2 vibrational modes such as 430 and 730 cm^{-1} appear only weakly in the z sublevel spectrum of thioxanthone. These vibrations are still of quite low intensity in the case of xanthone where ΔE_{TT} is much smaller than that of thioxanthone. This indicates that also the vibronic bands involving the a_2 vibrations should gain intensity by mechanism (3b) rather than (3a).

Radiative Decay from the y Sublevel: In the case of $^3\pi,\pi^*$ aromatic carbonyls, the y sublevel emission was ascribed to the direct mixing with the $^1\sigma,\pi^*$ state, largely localized on the carbonyl group[7,12]

$$T_y(^3\pi,\pi^*) \leftarrow H_{so} \rightarrow {}^1\sigma,\pi^*(B_1).$$

The y sublevel emission of xanthone has also been explained with this mechanism.[17]

In xanthone, however, the ether group participates in the π-conjugation. It is therefore necessary to consider the importance of one center terms on the O atom of the ether group in spin orbit coupling matrix element in addition to the above mechanism. The y sublevel is expected to couple with $^1B_1(\sigma',\pi^*)$, where σ' orbital has a large contribution from in-plane non-bonding orbital of sp^2 hybrid type in the ether group. Since the effective one electron spin orbit coupling constant for sulfur is much larger than for oxygen,[25] the contribution of the mixing with $^1B_1(\sigma',\pi^*)$ state is more important in thioxanthone than in xanthone. In fact, there is evidence that the radiative activity of the y sublevel increases dramatically in going from xanthone to thioxanthone as given in Table 2. In addition, the vibronic bands involving non-totally symmetric vibrations appear with some intensity in the y sublevel spectrum. It is likely that the vibronic interaction in singlet manifolds involving the $^1B_1(\sigma',\pi^*)$ and $^1\pi,\pi^*$ states is the main source for the emission in these bands, rather than the vibronic interaction in triplet manifolds.

The authors wish to thank Prof. Saburo Nagakura of the University of Tokyo and Prof. Nobuyuki Nishi of Institute for Molecular Science for their valuable discussions. The present work was in part supported by a Grant-in-Aid for Scientific Research from the Ministry of Education, Science and Culture (Nos. 334026, 410401).

References

1) A. H. Nishimura and J. S. Vincent, *Chem. Phys. Lett.*, **13**, 89 (1972).
2) A. H. Nishimura and D. S. Tinti, *Chem. Phys. Lett.*, **13**, 278 (1972).
3) T. H. Cheng and N. Hirota, *J. Chem. Phys.*, **50**, 5019 (1972).
4) C. R. Jones, D. R. Kearns, and A. H. Maki, *J. Chem. Phys.*, **50**, 873 (1973).
5) H. Hayashi and S. Nagakura, *Mol. Phys.*, **24**, 801 (1972); **27**, 969 (1974).
6) M. A. Souto, P. J. Wagner, and M. A. El-Sayed, *Chem. Phys.*, **6**, 193 (1974).
7) T. H. Cheng and N. Hirota, *Mol. Phys.*, **27**, 281 (1974).
8) E. T. Harrigan and N. Hirota, *Mol. Phys.*, **31**, 663, 681 (1976).
9) S. J. Sheng and M. A. El-Sayed, *Chem. Phys.*, **20**, 61 (1977).
10) T. Takemura and H. Baba, *Bull. Chem. Soc. Jpn.*, **44**, 2756 (1969).
11) W. A. Case and D. R. Kearns, *J. Chem. Phys.*, **52**, 2175 (1970).
12) Y. Tanimoto, H. Kobayashi, S. Nagakura, and T.

Azumi, *Chem. Phys. Lett.*, **16**, 10 (1972).
13) C. R. Jones, D. R. Kearns, and R. M. Wing, *J. Chem. Phys.*, **58**, 1370 (1973).
14) H. J. Pownall and J. R. Huber, *J. Am. Chem. Soc.*, **93**, 6429 (1971).
15) H. J. Pownall and I. Granoth, *J. Phys. Chem.*, **80**, 508 (1976).
16) H. J. Pownall and W. W. Mantulin, *Mol. Phys.*, **31**, 1393 (1976).
17) A. Chakrabarti and N. Hirota, *J. Phys. Chem.*, **80**, 2966 (1976).
18) R. E. Connors and P. S. Walsh, *Chem. Phys. Lett.*, **52**, 436 (1977).
19) T. Terada, M. Koyanagi, and Y. Kanda, *Chem. Phys. Lett.*, **80**, 508 (1980).
20) N. Nishi and M. Kinoshita, *Bull. Chem. Soc. Jpn.*, **49**, 1221 (1977).
21) E. Kanezaki, N. Nishi, and M. Kinoshita, *Bull. Chem. Soc. Jpn.*, **52**, 2836 (1979).
22) The $T_1 \leftarrow S_0$ absorptions of the host crystals are hidden in the strong absorption bands starting at about 24900 cm^{-1}.
23) J. Schmidt, D. A. Antheunis, and J. H. van der Waals, *Mol. Phys.*, **22**, 1 (1971).
24) D. A. Antheunis, J. Schmidt, and J. H. van der Waals, *Mol. Phys.*, **27**, 1571 (1974).
25) M. Blume and R. E. Watson, *Proc. R. Soc. London, Ser. A*, **270**, 127 (1962); **271**, 565 (1963).
26) T. L. Brown, *Spectrochim. Acta*, **18**, 1067 (1962).
27) E. D. Bergman and S. Pinchas, *J. Chem. Phys.*, **49**, 517 (1966).
28) F. M. Abdel-Kerin and H. A. Shoeb, *Z. Phys. Chem. (Leipzig)*, **251**, 209 (1972).